# Uric Acid Electroanalysis

Subjects: Medical Laboratory Technology

Contributor: Ligia Chelmea , Mihaela Badea , Ioan Scarneciu , Marius Alexandru Moga , Lorena Dima , Patrizia Restani , Cecilia Murdaca , Daniel Ciurescu , Laura Elena Gaman

Uric acid is a metabolic product that results from degradation of purines in the liver. Usually, uric acid is identified from biological fluids, human serum and urine through conventional methods, such as spectroscopy, chromatography, electrochemistry, membrane capillary electrophoresis and spectrophotometric methods, including uricase enzymatic reactions. Importantly, uric acid determination opens the possibility of early intervention in cases of hyperuricemia and preventing the degradation of renal function.

uric acid chemosensors biosensors nanocomposites

## 1. Introduction

From the electrochemical point of view, uric acid is a weak acid, with two-step dissociation at a $pKa_1$ of 5.4 and a $pKa_2$ of 9.8. In the physiological range of pH (7.35–7.45), in the extracellular compartment, uric acid is found mostly (98%) in the form of biurate (deprotonated urate anion or ionized urate), and a very small quantity (<1%) is found as undissociated uric acid [1]. However, in more acid pH media, such as urine (pH 6.5), uric acid is still found mainly as biurate (88%) but with an increased percentage as uric acid (12%) [1][2].

The physiological levels of uric acid are between 3.5 mg/dL and 7.2 mg/dL (210 µM and 430 µM) in males, and between 2.6 mg/dL and 6.0 mg/dL (155 µM and 360 µM) in premenopausal females [1]. These levels are maintained by exogenous input (diet) but mostly by endogenous formation (nucleic acid catabolism and de novo synthesis) [3].

At high levels of uric acid, hyperuricemia, the undissociated uric acid precipitates at the vascular level and biurate is implicated in kidney stones formation. This phenomenon occurs because of the low solubility (6 mg/dL or 360 µM) of uric acid, mainly in the form of monosodium urate [1].

The oxidation of uric acid starts with the formation of diimine (a) by exchanging $2e^-$ and $2H^+$. The resulting diimine takes up two molecules of water and forms imine-alcohol (b) and uric acid-4,5-diol (c), successively. Ultimately, uric acid-4,5-diol is decomposed to allantoin (d) and $CO_2$ in neutral pH (**Figure 1**) [4].

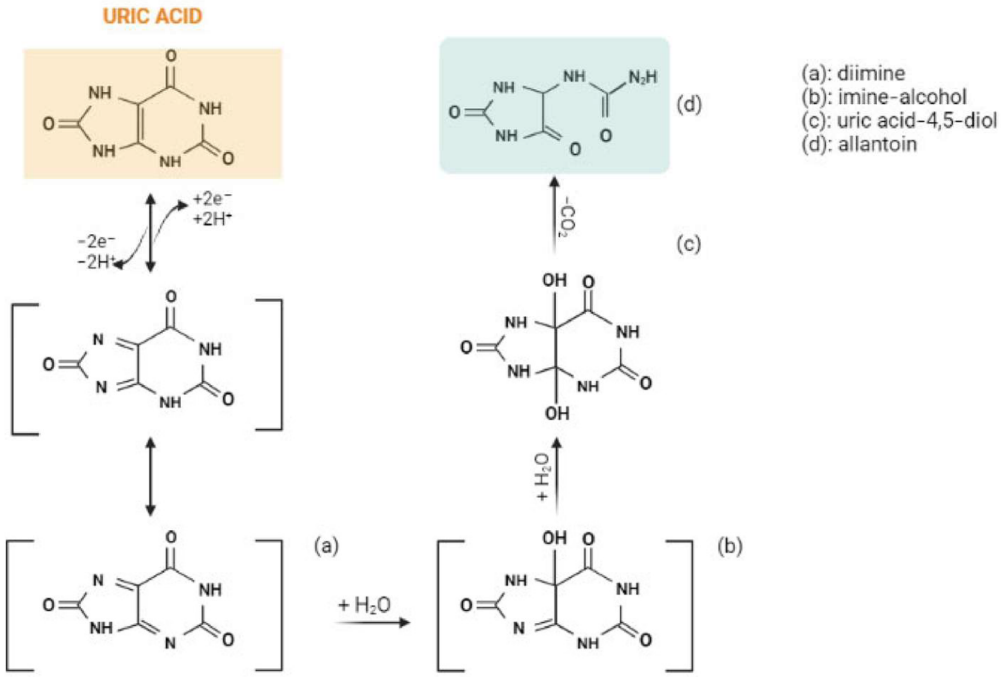


**Figure 1.** The electrochemical oxidation of uric acid to allantoin. Created with BioRender.com.

The oxidative properties of uric acid can be used in developing catalytic methods of detection. Thanks to the high electrochemical capacity of uric acid, for the rapid quantification of uric acid levels, scientists have developed different uric acid detection tools.

Together with uric acid, dopamine and ascorbic acid have similar oxidative behavior and coexist in urine samples [5]. Therefore, uric acid, dopamine and ascorbic acid signals can interfere with each other in the process of electrochemical detection in real samples. These three compounds have a very similar oxidation potential, so their electrochemical detection is very challenging [5] as obtaining separate voltametric peaks is the principal objective [6]. This matter has been investigated frequently for most types of electrodes, such as conventional sensors, modifiable electrodes and biosensors.

However, dopamine, uric acid and ascorbic acid have individual and cumulative importance because of their role in oxidative stress-related diseases [7]. Parkinson's disease, most of all, lacks a rapid diagnostic method using biological markers for diagnosis of the early stages of the pathology [8] and it is an example where simultaneous detection of the three compounds may be useful [9].

Other cases in which it may be important to establish levels of uric acid and its electrochemically similar compounds, dopamine and ascorbic acid, in biological matrixes are the following: dopamine: cardiotoxicity [10], aging [11], multiple sclerosis [12], rheumatoid arthritis [12], Alzheimer's disease [12], and Tourette [12]; uric acid: arthritis [13], gout [13], Lesch–Nyhan syndrome [13], urolithiasis [13], kidney damage [13], leukemia [14], lymphoma [14], and multiple sclerosis [15]; and ascorbic acid: high blood pressure [16], heart attack risk [16], cataracts [16], tooth decay [16], improper bone development [16], loss of appetite [16], weakened cartilage [16], skin hemorrhages [16], impaired digestion [16], septic shock [17], and diabetes mellitus [18].

## 2. Uric Acid Electrochemical Detection

Among the transition metal oxide-modified electrodes, ZnO NWAs/GF/GCE [19] had the best performance in terms of sensitivity, but highly selective sensors with moderately higher limits of detection included GCE/MC–GO–$Fe_3O_4$ [20], CuO/GCE [21] and RuON-GCE [22] (**Table 1**).

**Table 1.** Comparison of electrodes modified with transition metal nanoparticles for detection of uric acid.

| Electrode | Technique | pH | Interference | Biological Sample; Relative Recovery (RR) | UA Linear Range (μM) | UA LOD (μM) | Ref. |
|---|---|---|---|---|---|---|---|
| GCE/MC–GO–$Fe_3O_4$ [1] | CV, DPV | 7.0 | UA, AA, DA, G, sucrose, L-Cys, citric acid, $Fe^{2+}$, $Cl^-$, $Na^+$, $NO_3^-$ | Human urine RR > 96% | 0.5–140 | 0.17 | [20] |
| $TiO_2$ NPs/GCE [2] | DPV | 7.0 | UA | Human urine RR: 97–99.6% | 1–9 | 0.764 | [23] |
| PdNPs/rGO/GCE [3] | DPV | 7.2 | UA, AA, DA | Human serum RR: 96.6–108.5% | 0.3–1400 | 16.67 | [24] |
| $SnO_2$/chitosan/GCE [4] | DPV | | UA, AA, DA | Human urine RR: 97.4% | 3–200 | 1 | [25] |
| CuO/GCE [5] | CV | 7.4 | UA, UR, lactic acid, ethanol, G, $K^+$, $Na^+$ | Human urine RR: 95–104% | 0.001–351,000 | 0.6 | [21] |
| RuON-GCE [6] | DPV | 7.0 | UA, E | Human urine RR: 98–101.6% | 3.0–56.6; 56.6–758.6 | 0.47 | [22] |
| $MoS_2$ NSA/CNFs [7] | CV, DPV | 7.0 | UA, levodopa | Human urine RR: 99.7–102.6% | 1–60 | 1 | [26] |
| CuO nano-rice/GCE [8] | CV, DPV | 7.0 | UA, AA, DA, G, fructose, galactose, lactose, $Na^+$, $Cl^-$, $K^+$, $Ca^{2+}$, $Br^-$, | Human urine | 1–60 | 1.2 | [27] |

| Electrode | Technique | pH | Interference | Biological Sample; Relative Recovery (RR) | UA Linear Range (μM) | UA LOD (μM) | Ref. |
|---|---|---|---|---|---|---|---|
| | | | $CO_2^{3-}$, $NH4^+$, $NO_2^-$, $NO_3^-$, $SO_4^{2-}$, $SO_3^{2-}$ [29] | RR: 98.6–102.6% | 8 [30] | | [31] |
| $Fe_3O_4$@CNT-N/GCE [9] | SWV | [33] 2.5 [29] | UA, AA, DA | [34] - | 25–85 | [29] 0.47 | [28] |
| ZnO NWAs/GF/GCE [10] | DPV | 7.4 | UA, AA, DA | Human serum | 0–40 | 0.001 | [19] |

| Electrode | Technique | pH | Interference | Biological Sample. Relative Recovery (RR) | UA Linear Range (μM) | UA LOD (μM) | Ref. |
|---|---|---|---|---|---|---|---|
| GO/AuNR/GCE [1] | DPV | - | UA, AA, DA, G, UR, $Mg^{2+}$ | Human urine | 10–90 | 0.4 | [31] |
| AuNPs@GO/PPy/CFP [2] | DPV | 7.0 | UA, AA, DA | Human urine RR: 96.8–109% | 2–360 | 1.68 | [35] |
| AuNPs-GO/Au-IDA [3] | CV | 7.0 | UA, AA, DA, G, E | Human urine | 2–1050 | 0.62 | [36] |
| GCE-PErGO-AuNP [4] | CV, DPV | 7.4 | UA, AA, DA | Human urine | 20–260 | 20 | [33] |
| AuRGO/GCE [5] | DPV | 7.0 | UA, AA, DA | Human serum RR: 97.5–102% | 88–53 | 1.8 | [37] |
| Au@Pd-RGO/GCE [6] | DPV | 7.0 | UA, AA, DA | Human urine RR: 97.1–102.5% | 0.02–500; 0.1–350 | 0.005; 0.02 | [29] |
| PEI/[$P_2W_{16}V_2$-Au/PDDA-rGO]$_8$ [7] | DPV | 7.0 | UA, AA, DA, NaCl, KCl, $NH_4Cl$, L-Cys, L-Glu, CA, UR, G | Human urine RR: 95.2–103.1% | 0.25–1500 | 0.08 | [30] |
| rGO-PAMAM-CNT-Au [8] | DPV | 4.0 | UA, AA, DA | - | 1–114 | 0.33 | [38] |
| Naf/AuNPs/AzA/MWCNTs [9] | DPV | 7.0 | UA, AA, DA, Trp, $Na^+$, $K^+$, $Ca^{2+}$, | Human urine | 0.5–50 | 0.28 | [34] |

| Electrode | Technique | pH | Interference | Biological Sample. Relative Recovery (RR) | UA Linear Range (μM) | UA LOD (μM) | Ref. |
|---|---|---|---|---|---|---|---|
| | | | $Mg^{2+}$, G, citric acid, tartaric acid | RR: 99.7–103% | | | |
| ITO-rGO-AuNPs [10] | LSV | 8.0 | UA, AA, Cl, $Na^+$, $Ca^{2+}$ $NH_4^+$ | Human urine, milk | 10–500 [13] | 3.6 | [39] |
| EGFET-AuE [11] [42] | - | 7.0 | UA, AA, G, bilirubin, hemoglobin | Human urine, serum | [41] 1–1000 | 0.5 | [15] |

**Table 3.** Comparison of different GMES for detection of uric acid.

| Electrode | Technique | pH | Interference | Biological Sample; Relative Recovery (RR) | UA Linear Range (μM) | UA LOD (μM) | Ref. |
|---|---|---|---|---|---|---|---|
| ZIF-11/GCE [1] | DP-ASV | 7.0 | UA, AA, G, sodium benzoate, saccharine, XA, hypoxanthine, KCl, $Na_2CO_3$, $Na_2SO_4$, $CaCO_3$ | Human urine RR: 94.5–104.4% | 50–540 | 0.48 | [13] |
| NgB/CPE [2] | CV, DPV | 7.0 | UA, AA, DA | Human urine RR: 99.4–100.4% | 12.5–750 | 5 | [48] |
| ErGO/PEDOT:PSS/GCE [3] | DPV | - | UA, DA | Human urine RR: 96.8–109% | 10–100 | 1.08 | [49] |
| PMES/RGO/GCE [4] | CV | 7.0 | UA, AA, DA, L-Cys, L-Lys, L-Tyr, G | Human urine | 0.1–100 | 0.056 | [50] |

AA = ascorbic acid, CA = citric acid, Cys = cysteine, DA = dopamine, E = epinephrine, G = glucose, Glu = glutamate, LSV = linear sweep voltammetry, Trp = tryptophan, UA = uric acid, UR = urea. [1] = Gold nanorod-decorated graphene oxide glassy carbon electrode; [2] = Gold nanoparticles-decorated polypyrole/graphene oxide nanosheets; [3] = Gold interdigitated microelectrodes array modified with graphene oxide and doped with gold nanoparticles; [4] = Gold nanoparticles deposition on reduced graphene oxide based on glassy carbon electrode; [5] = Reduced graphene oxide and gold nanoplates modified glassy carbon electrode; [6] = Reduced graphene oxide-supported bimetallic, gold-palladium nanocomposites; [7] = Poly(diallyldimethylammonium chloride)-functionalized

| Electrode | Technique | pH | Interference | Biological Sample; Relative Recovery (RR) | UA Linear Range (μM) | UA LOD (μM) | Ref. |
|---|---|---|---|---|---|---|---|
| | | | | RR: 103.35% | | | |
| NG/GCE [5] | DPV | 6.0 | UA, AA, DA | - | 0.1–20 | 0.045 | [51] |
| MC/GCE [6] | CV, DPV | 1.0 | UA, AA, DA | Synthetic urine RR: 101% | 10–150 | 1.7 | [52] |
| BDG-based electrode [7] | SWV | 2.25 | UA | Human urine RR: 95% RR: 95.2–103.1% | 8–1000 | 7.7 | [53] |
| PMB-ERGO/GCE [8] | SWV | 3.0 | UA, XA | Human urine RR: 97.8% | 0.08–400 | 0.03 | [14] |
| PEDOT-nf/PGE and Ox-PEDOT-nf/PGE [9] | CV | 2.0 | UA | Human urine, serum RR: 104–107% | 0.1–20 | 0.0013 | [41] |
| MWNTs/MGF/GCE [10] | DPV | 7.3 | UA, AA, DA, Trp, $Na^+$, $K^+$, $Ca^{2+}$, $Mg^{2+}$, G | - | 5–100; 300–10,000 | 0.93 | [9] |
| GCE/tosyl-CNPsE [11] | CV | 2.0 | UA, AA | Human urine RR: 106% | 0.1–100 | 0.2 | [42] |
| CTAB/GO/MWNTs/GCE [12] | DPV | 7.0 | UA, AA, DA, $NO_2^-$ | Human urine RR: 99–115% | 3–600 | 1 | [40] |
| EGNWsE [13] | DPV | 7.4 | UA, AA, DA | - | 2.6–200 | 0.000033 | [54] |
| GEF/CFE [14] | DPV | 7.0 | UA, AA, DA | Human urine, | 3.98–371 | 2 | [55] |

| Electrode | Technique | pH | Interference | Biological Sample; Relative Recovery (RR) | UA Linear Range (μM) | UA LOD (μM) | Ref. |
|---|---|---|---|---|---|---|---|
| | | | | serum | | | |
| Trp-GR/GCE [15] | DPV | 7.0 | UA, AA, DA [64][65] | Human urine RR: 97.3–99.9% Human serum RR: 92.6–98.7% [67][68][69][70] | 10–1000 | 1.24 [66] | [56] |
| $NH_2$-VMSF/ErGO/SPCE [16] | DPV [66] | 5.0 | UA, AA, DA, G, UR, $Na^+$, $K^+$, $Ca^{2+}$, $Mg^{2+}$ [66] | Human whole blood RR: 99.0–107.0% | 0.5–180 [73] | 0.129 | [57] |

[3] [71] [72]

The scientific literature [74] also mentions different approaches and emerging strategies to develop reliable biosensors that consider different active and passive anti-biofouling strategies (**Figure 2**), thereby extending their applications to biological samples for clinical diagnostics, personalized medicine, point-of-care testing, and wearable devices.

AA = ascorbic acid; DA = dopamine; G = glucose; L-Cys = L-cystine; L-Lys = L-lysine; L-Tyr = L-tyrosine; SWV = square wave voltammetry; Trp = tryptophan; UA = uric acid; UR = urea; XA = xanthine; [1] = Zeolite Imidazolate Framework-11-modified electrode; [2] = Poly (Naphthol Green B)-film-modified carbon paste electrode; [3] = Gold nanoparticle-decorated polypyrrole/graphene oxide nanosheets; [4] = Poly(2-(N-morpholine)ethane sulfonic acid)/RC [5] [6] [7] n-doped diamonc [8] ite film-modified [9] graphite electrod [10] (MGF) nanocor [11] s/glassy carbon e [12] D)/multi-walled c [13] fied 'as-grown' e raphene flowers; [15] [16] lectrode equipped with vertically-ordered mesoporous silica-nanochannel film.

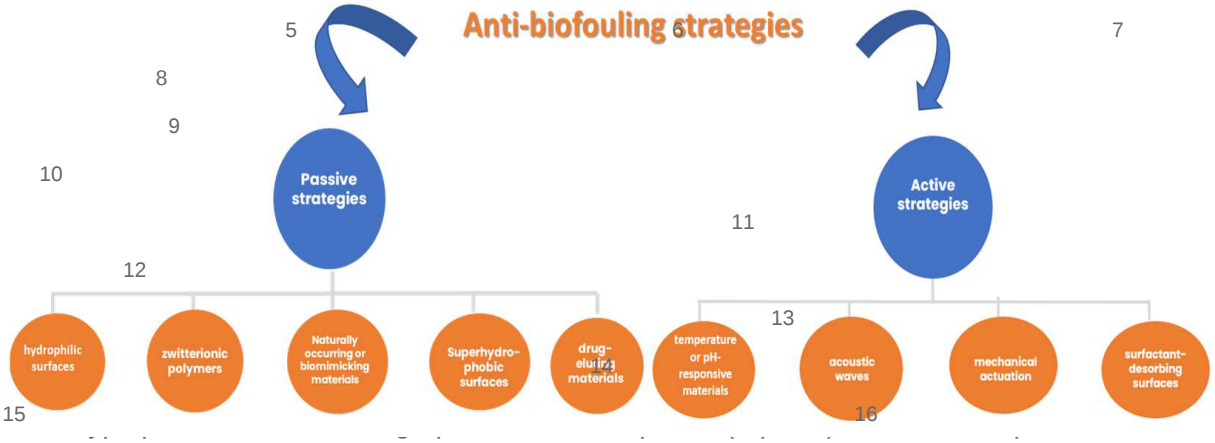


**Figure 2.** Anti-biofouling strategies.

**Table 4.** Comparison of biosensors for detection of uric acid.

The abovementioned anti-biofouling strategies aim to delay the biofouling process and remove the accumulation of different bioactive compounds, if necessary. There is also the possibility of using combinations of different materials (materials with natural morphology and surface stability) and transducers to achieve a better long-term reliability.

| Electrode | Technique | pH | Interference | Biological Sample. Relative Recovery (RR) | UA Linear Range (μM) | UA LOD (μM) | Ref. |
|---|---|---|---|---|---|---|---|
| UOx/CNT/CMC [1] | CV | 7.4 | UA, AA, UR | Human urine, serum RR: 96.3% | 20–5000 | 2.8 | [46] |
| RGO/AuNP hybrid film [2] | Amperometry | 7.6 | UA, AA, DA | - | - | 1 | [58] |
| UOx-Th-SWNTs/GC [3] | - | - | UA, AA, 3,4-dihydroxyphenylacetic acid, 4-acetamidophenol | HEK 293A cells RR: 100.9–101.4% | 2–2000 | 0.5 | [59] |
| UOx/PBG/CNT/CFE and UOx PTH/CNT/CFE [4] | Amperometry | 7.0 | UA, AA, G, citric acid, creatinine, $NH_4^+$, phenol, UR | Human urine RR: 95–105% | 2–100 | 0.6 | [44] |
| UOx/rGO/ZnPc-$NH_2$/GCE [5] | - | - | UA | Human urine RR: 92.5–97.6% | 0.5–100 | 0.15 | [43] |
| MP/SWCNT/SPE [6] | CV | 7.4 | UA, AA, DA | Human urine | 0.001–0.20 | 0.83 | [45] |
| UOx/AuNP/c-MWCNT/Au [7] | CV | 7.5 | UA, AA, G, chol, UR, pyruvate, bilirubin, $CuSO_4$, KCl, FAD, NaCl, $ZnSO_4$, NADH, $CaCl_2$, EDTA, NEM, riboflavin, $MnCl_2$, FM | Human serum RR: 95–97% | 5–800 | 5 | [47] |
| UOx- PANI-PB-PtE [8] | CV | 7.2 | UA, AA, UR, G | Human serum | 10–160 | 2.6 | [60] |
| UOx-PANI-MWCNT/ITO [9] | CV, DPV | - | UA | Human serum | 10–1000 | 10 | [61] |
| UOx/Nafion/ZnO-NFs/Au [10] | Amperometry | 7.4 | UA, AA, UR, G | - | 0.5–1500 | 0.5 | [62] |
| Naf/UOx/Fc/GCE [11] | DPV, Amperometry | 7.4 | UA, AA, DA, UR, G, XA | Human serum RR: 95% | 0.5–50; | 0.23 | [63] |

production in T cells, and abnormalities in the dopaminergic system in T cells in autoimmune, neurological and psychiatric diseases. Acta Physiol. 2016, 216, 42–89.

| Electrode | Technique | pH | Interference | Biological Sample. Relative Recovery (RR) | UA Linear Range (μM) | UA LOD (μM) | Ref. |
|---|---|---|---|---|---|---|---|
| 1 | | | | | | | ; Tuyen, dazolate |
| 1 | | | | | 25–600 | | anthine m |

AA = ascorbic acid, Chol = cholesterol, DA = dopamine, G = glucose, UA = uric acid, UR = urea. [1] = Uricase/carbon nanotube/carboxymethylcellulose electrode; [2] = Large-scale graphene film doped with gold nanoparticles; [3] = uricase − thionine − single-walled carbon nanotube-modified electrodes; [4] = Poly(brilliant green) and poly(thionine)-modified carbon nanotube-coated carbon film electrode; [5] = Zinc tetraaminophthalocyanine-functionalized graphene nanosheets/GCE with UA; [6] = Multi-walled carbon nanotubes (MWCNTs) and polyaniline (PANI) layer, electrochemically deposited on the surface of Au electrode; [8] = Uricase-immobilized Polyaniline/Prussian blue (PANI-PB) composite on a platinum electrode (PtE); [9] = Uricase immobilized onto multi-walled carbon nanotubes (CNT) doped polyaniline (PANI) nanocomposite-indium tin oxide (ITO)-coated glass substrate; [10] = Uricase immobilized in conjunction with Nafion onto zinc oxide nanoflakes (ZnO-NF) and a gold-coated glass substrate; [11] = Ferrocene (Fc)-induced electro-activated uricase (UOx) deposited within Nafion (Naf) on glassy carbon electrode (GCE).


15. Guan, W.; Duan, X.; Reed, M.A. Highly specific and sensitive non-enzymatic determination of uric acid in serum and urine by extended gate field effect transistor sensors. Biosens. Bioelectron. 2014, 51, 225–231.
16. Thadeus, A.; Subramaniam, P.A.; Weldu, A.; Agarwal, R. Electrochemical determination and comparison of ascorbic acid in freshly prepared and bottled fruit juices (Fanta®) using cyclic voltammetric study. J. Chem. Pharm. Res. 2014, 6, 880–888.
17. Carr, A.C.; Shaw, G.M.; Fowler, A.A.; Natarajan, R. Ascorbate-dependent vasopressor synthesis: A rationale for vitamin C administration in severe sepsis and septic shock? Crit. Care 2015, 19, 418.
18. Ide, K.; Yamada, H.; Umegaki, K.; Mizuno, K.; Kawakami, N.; Hagiwara, Y.; Matsumoto, M.; Yoshida, H.; Kim, K.; Shiosaki, E.; et al. Lymphocyte vitamin C levels as potential biomarker for progression of Parkinson's disease. Nutrition 2015, 31, 406–408.
19. Yue, H.Y.; Huang, S.; Chang, J.; Heo, C.; Yao, F.; Adhikari, S.; Gunes, F.; Liu, L.C.; Lee, T.H.; Oh, E.S.; et al. ZnO Nanowire arrays on 3D hierachical graphene foam: Biomarker detection of Parkinson's disease. ACS Chem. Neurosci. 2014, 8, 1639–1646.
20. Sohouli, E.; Khosrowshahi, E.M.; Radi, P.; Naghian, E.; Rahimi-Nasrabadi, M.; Ahmadi, F. Electrochemical sensor based on modified methylcellulose by graphene oxide and Fe3O4 nanoparticles: Application in the analysis of uric acid content in urine. J. Electroanal. Chem. 2020, 877, 114503.
21. Buledi, J.; Ameen, S.; Memon, S.; Fatima, A.; Solangi, A.; Mallah, A.; Karimi, F.; Malakmohammadi, S.; Agarwal, S.; Gupta, V. An Improved Non-Enzymatic Electrochemical Sensor Amplified with CuO Nanostructures for Sensitive Determination of Uric Acid. Open. Chem. 2021, 19, 481–491.
22. Zare, H.R.; Ghanbari, Z.; Nasirizadeh, N.; Benvidi, A. Simultaneous Determination of Adrenaline, Uric Acid, and Cysteine Using Bifunctional Electrocatalyst of Ruthenium Oxide Nanoparticles. Comptes Rendus Chim. 2013, 3, 287–295.
23. Rajeswari, B.; Reddy, K.V.N.S.; Devi, A.S.; Madhavi, G.; Reddy, I.R.V.S. Determination of Uric Acid Using TiO2 Nanoparticles Modified Glassy Carbon Electrode. Biointerface Res. Appl. Chem. 2022, 12, 6058–6065.

24. Wei, Y.; Liu, Y.; Xu, Z.; Wang, S.; Chen, B.; Zhang, D.; Fang, Y. Simultaneous Detection of Ascorbic Acid, Dopamine, and Uric Acid Using a Novel Electrochemical Sensor Based on Palladium Nanoparticles/Reduced Graphene Oxide Nanocomposite. Int. J. Anal. Chem. 2020, 2020, 8812443.
25. Sun, D.; Zhao, Q.; Tan, F.; Wang, X.; Gao, J. Simultaneous Detection of Dopamine, Uric Acid, and Ascorbic Acid Using SnO2 Nanoparticles/Multi-Walled Carbon Nanotubes/Carbon Paste Electrode. Anal. Methods 2012, 10, 3283.
26. Wang, W.Q.; Yue, H.Y.; Yu, Z.M.; Huang, S.; Song, S.S.; Gao, X.; Guan, E.H.; Zhang, H.J.; Wang, Z. Synthesis and Application of MoS2 Nanosheet Arrays/Carbon Nanofibers for Simultaneous Electrochemical Determination of Levodopa and Uric Acid. IEEE Sens. J. 2019, 15, 5988–5994.
27. Krishnamoorthy, K.; Sudha, V.; Kumar, S.M.S.; Thangamuthu, R. Simultaneous Determination of Dopamine and Uric Acid Using Copper Oxide Nano-Rice Modified Electrode. J. Alloys Compd. 2018, 748, 338–347.
28. Fernandes, D.M.; Costa, M.; Pereira, C.; Bachiller-Baeza, B.; Rodriguez-Ramos, I.; Guerrero-Ruiz, A.; Freire, C. Novel electrochemical sensor based on N-doped carbon nanotubes and Fe3O4 nanoparticles: Simultaneous voltammetric determination of ascorbic acid, dopamine and uric acid. J. Colloid Interface Sci. 2014, 432, 207–213.
29. Jiang, J.; Du, X. Sensitive Electrochemical Sensors for Simultaneous Determination of Ascorbic Acid, Dopamine, and Uric Acid Based on Graphene Oxide Nanocomposites. Nanoscale 2014, 19, 11303–11309.
30. Bai, Z.; Zhou, C.; Xu, H.; Wang, G.; Pang, H.; Ma, H. Polyoxometalates-Doped Au Nanoparticles and Reduced Graphene Oxide: A New Material for the Detection of Uric Acid in Urine. Sens. Actuators B Chem. 2017, 243, 361–371.
31. Safitri, H.; Wahyuni, W.T.; Rohaeti, E.; Khalil, M.; Marken, F. Optimization of uric acid detection with Au nanorod-decorated graphene oxide (GO/AuNR) using response surface methodology. RSC Adv. 2022, 12, 25269–25278.
32. Liu, K.; Zhang, J.; Yang, G.; Wang, C.; Zhu, J.-J. Direct Electrochemistry and Electrocatalysis of Hemoglobin Based on Poly(Diallyldimethylammonium Chloride) Functionalized Graphene Sheets/Room Temperature Ionic Liquid Composite Film. Electrochem. Commun. 2010, 3, 402–405.
33. Imran, H.; Palinci, N.M.; Venkataraman, D. Facile and Green Synthesis of Graphene Oxide by Electrical Exfoliation of Pencil Graphite and Gold Nanoparticle for Non-Enzymatic Simultaneous Sensing of Ascorbic Acid, Dopamine and Uric Acid. RSC Adv. 2015, 78, 63513–63520.
34. Filik, H.; Avan, A.A.; Aydar, S. Simultaneous Detection of Ascorbic Acid, Dopamine, Uric Acid and Tryptophan with Azure A-Interlinked Multi-Walled Carbon Nanotube/Gold Nanoparticles

Composite Modified Electrode. Arab. J. Chem. 2016, 3, 471–480.

35. Tan, C.; Zhao, J.; Sun, P.; Zheng, W.; Cui, G. Gold Nanoparticle Decorated Polypyrrole/Graphene Oxide Nanosheets as a Modified Electrode for Simultaneous Determination of Ascorbic Acid, Dopamine and Uric Acid. New. J. Chem. 2020, 12, 4916–4926.
36. Abellán-Llobregat, A.; Vidal, L.; Rodríguez-Amaro, R.; Berenguer-Murcia, A.; Canals, A.; Morallón, E. Au-IDA Microelectrodes Modified with Au-Doped Graphene Oxide for the Simultaneous Determination of Uric Acid and Ascorbic Acid in Urine Samples. Electrochim. Acta 2017, 227, 275–284.
37. Wang, C.; Du, J.; Wang, H.; Zou, C.; Jiang, F.; Yang, P.; Du, Y. A Facile Electrochemical Sensor Based on Reduced Graphene Oxide and Au Nanoplates Modified Glassy Carbon Electrode for Simultaneous Detection of Ascorbic Acid, Dopamine and Uric Acid. Sens. Actuators B Chem. 2014, 204, 302–309.
38. Wang, S.; Zhang, W.; Zhong, X.; Chai, Y.; Yuan, R. Simultaneous Determination of Dopamine, Ascorbic Acid and Uric Acid Using a Multi-Walled Carbon Nanotube and Reduced Graphene Oxide Hybrid Functionalized by PAMAM and Au Nanoparticles. Anal. Methods 2015, 4, 1471–1477.
39. Mazzara, F.; Patella, B.; Ganci, F.; O'Riordan, A.; Aiello, G.; Torino, C.; Vilasi, A.; Sunseri, C.; Inguanta, R. Flexible Electrode Based on Gold Nanoparticles and Reduced Graphene Oxide for Uric Acid Detection Using Linear Sweep Voltammetry. Chem. Eng. Trans. 2021, 87, 421–426.
40. Yang, Y.J.; Li, W. CTAB functionalized graphene oxide/multiwalled carbon nanotube composite modified electrode for the simultaneous determination of ascorbic acid, dopamine, uric acid and nitrite. Biosens. Bioelectron. 2014, 56, 300–306.
41. Ozcan, A.; Ilkbas, S. Preparation of poly(3,4-ethylenedioxythiophene) nanofibers modified pencil graphite electrode and investigation of over-oxidation conditions for the selective and sensitive determination of uric acid in body fluids. Anal. Chim. Acta 2015, 891, 312–320.
42. Amiri, M.; Imanzadeh, H.; Banaei, A. Carbon nanoparticles with tosyl functional group for distinguishing voltammetric peaks of ascorbic acid and uric acid. Mater. Sci. Eng. 2015, C47, 189–195.
43. Shi, Y.-M.; Mei, L.; Zhang, J.-X.; Hu, K.; Zhang, X.; Li, Z.-Z.; Miao, M.-S.; Li, X.-M. Synthesis of Zinc Tetraaminophthalocyanine Functionalized Graphene Nanosheets as an Enhanced Material for Sensitive Electrochemical Determination of Uric Acid. Electroanalysis 2020, 7, 1507–1515.
44. Ghica, M.E.; Brett, C.M.A. Poly(brilliant green) and poly(thionine) modified carbon nanotube coated carbon film electrodes for glucose and uric acid biosensors. Talanta 2014, 130, 198–206.
45. Herrastia, Z.; Martíneza, F.; Baldrich, E. Detection of uric acid at reversibly nanostructured thin-film microelectrodes. Sens. Actuators 2016, B234, 667–673.

46. Fukuda, T.; Muguruma, H.; Iwasa, H.; Tanaka, T.; Hiratsuka, A.; Shimizu, T.; Tsuji, K.; Kishimoto, T. Electrochemical Determination of Uric Acid in Urine and Serum with Uricase/Carbon Nanotube/Carboxymethylcellulose Electrode. Anal. Biochem. 2020, 590, 113533.
47. Rawal, R.; Chawla, S.; Chauhan, N.; Dahiya, T.; Pundir, C.S. Construction of amperometric uric acid biosensor based on uricase immobilized on PBNPs/cMWCNT/PANI/Au composite. Int. J. Biol. Macromol. 2012, 50, 112–118.
48. Chitravathi, S.; Kumara Swamy, B.E.; Mamatha, G.P.; Sherigara, B.S. Electrochemical Behavior of Poly (Naphthol Green B)-Film Modified Carbon Paste Electrode and Its Application for the Determination of Dopamine and Uric Acid. J. Electroanal. Chem. 2012, 667, 66–75.
49. Gao, N.; Yu, J.; Tian, Q.; Shi, J.; Zhang, M.; Chen, S.; Zang, L. Application of PEDOT:PSS and Its Composites in Electrochemical and Electronic Chemosensors. Chemosensors 2021, 9, 79.
50. Zhang, K.; Zhang, N.; Zhang, L.; Wang, H.; Shi, H.; Liu, Q. Simultaneous voltammetric detection of dopamine, ascorbic acid and uric acid using a poly(2-(N-morpholine)ethane sulfonic acid)/RGO modified electrode. RSC Adv. 2018, 8, 5280–5285.
51. Sheng, Z.-H.; Zheng, X.-Q.; Xu, J.-Y.; Bao, W.-J.; Wang, F.-B.; Xia, X.-H. Electrochemical sensor based on nitrogen doped graphene: Simultaneous determination of ascorbic acid, dopamine and uric acid. Biosens. Bioelectron. 2012, 34, 125–131.
52. Rattanaumpa, T.; Maensiri, S.; Ngamchuea, K. Microporous carbon in the selective electro-oxidation of molecular biomarkers: Uric acid, ascorbic acid, and dopamine. RSC Adv. 2022, 12, 18709–18721.
53. Cinkova, K.; Kianičkova, K.; Stanković, D.M.; Vojs, M.; Marton, M.; Švorc, Ľ. The doping level of boron-doped diamond electrodes affects the voltammetric sensing of uric acid. Anal. Methods 2018, 10, 991–996.
54. Roy, P.K.; Ganguly, A.; Yang, W.K.; Wu, C.T.; Hwang, J.S.; Tai, Y.; Chen, K.H.; Chen, L.C.; Chattopadhyay, S. Edge promoted ultrasensitive electrochemical detection of organic bio-molecules on epitaxial graphene nanowalls. Biosens. Bioelectron. 2015, 70, 137–144.
55. Du, J.; Yue, R.; Ren, F.; Yao, Z.; Jiang, F.; Yang, P.; Du, Y. Novelgraphene flowersmodified carbon fibers for simultaneous determination of ascorbic acid, dopamine and uric acid. Biosens. Bioelectron. 2014, 53, 220–224.
56. Lian, Q.; He, Z.; He, Q.; Luo, A.; Yan, K.; Zhang, D.; Lu, X.; Zhou, X. Simultaneous determination of ascorbic acid, dopamine and uric acid based on tryptophan functionalized graphene. Anal. Chim. Acta 2014, 823, 32–39.
57. Sayyad, P.W.; Sontakke, K.S.; Farooqui, A.A.; Shirsat, S.M.; Tsai, M.-L.; ShirsaT, M.D. A Novel Three-Dimensional Electrochemical Cd(II) Biosensor Based on l-Glutathione Capped Poly(3,4-

Ethylenedioxythiophene):Polystyrene Sulfonate/Carboxylated Multiwall CNT Network. J. Sci. Adv. Mater. Devices 2022, 7, 100504.

58. Zhang, P.; Huang, Y.; Lu, X.; Zhang, S.; Li, J.; Wei, G.; Su, Z. One-Step Synthesis of Large-Scale Graphene Film Doped with Gold Nanoparticles at Liquid–Air Interface for Electrochemistry and Raman Detection Applications. Langmuir. 2014, 30, 8980–8989.
59. Chen, D.; Wang, Q.; Jin, J.; Wu, P.; Wang, H.; Yu, S.; Zhang, H.; Cai, C. Low-potential detection of endogenous and physiological uric acid at uricase − thionine − single-walled carbon nanotube modified electrodes. Anal. Chem. 2010, 82, 2448–2455.
60. Thakur, B.; Sawant, S.N. Polyaniline/Prussian-Blue-Based Amperometric Biosensor for Detection of Uric Acid. ChemPlusChem 2012, 2, 166–174.
61. Arora, K.; Choudhary, M.; Malhotra, B.D. Enhancing performance of uricase using multiwalled carbon nanotube doped polyaniline. Appl. Biochem. Biotechnol. 2014, 174, 1174–1187.
62. Usman, A.S.M.; Ibupoto, Z.H.; Kashif, M.; Hashim, U.; Willander, M. A potentiometric indirect uric acid sensor based on ZnO nanoflakes and immobilized uricase. Sensors 2012, 12, 2787–2797.
63. Ghoh, T.; Sarkar, P.; Turner, A.P.F. A novel third generation uric acid biosensor using uricase, electro-activated with ferrocene on a Nafion coated glassy carbon electrode. Bioelectrochemistry 2015, 102, 1–9.
64. Hwang, C.; Lee, W.J.; Kim, S.D.; Park, S.; Kim, J.H. Recent Advances in Biosensor Technologies for Point-of-Care Urinalysis. Biosensors 2022, 12, 1020.
65. Irkham, I.; Ibrahim, A.U.; Pwavodi, P.C.; Al-Turjman, F.; Hartati, Y.W. Smart Graphene-Based Electrochemical Nanobiosensor for Clinical Diagnosis: Review. Sensors 2023, 23, 2240.
66. Balogun, S.A.; Fayemi, O.E. Recent Advances in the Use of CoPc-MWCNTs Nanocomposites as Electrochemical Sensing Materials. Biosensors 2022, 12, 850.
67. Li, Q.; Wang, Z.; Liang, Q.; Zhou, M.; Xu, S.; Li, Z.; Sun, D. Tetra-substituted cobalt (II) phthalocyanine/multi-walled carbon nanotubes as new efficient catalyst for the selective oxidation of styrene using tert-butyl hydroperoxide. Fuller. Nanotub. Carbon. Nanostruct. 2020, 28, 799–807.
68. Şavk, A.; Özdil, B.; Demirkan, B.; Nas, M.S.; Calimli, M.H.; Alma, M.H.; Asiri, A.M.; Şen, F. Multiwalled carbon nanotube-based nanosensor for ultrasensitive detection of uric acid, dopamine, and ascorbic acid. Mater. Sci. Eng. C 2019, 99, 248–254.
69. Wu, B.; Yeasmin, S.; Liu, Y.; Cheng, L.J. Ferrocene Functionalized Gold Nanoparticles on Carbon Nanotube Electrodes for Portable Dopamine Sensor. In Proceedings of the Electrochemical Society Meeting Abstracts 239, Digital Meeting, 30 May–3 June 2021; Volume 55, p. 1345.

70. Musarraf, H.M.; Asiri, A.M.; Uddin, J.; Marwani, H.M.; Rahman, M.M. Development of a L-cysteine Sensor Based on Thallium Oxide Coupled Multi-walled Carbon Nanotube Nanocomposites with Electrochemical Approach. Chem. Asian J. 2022, 17, e202101117.
71. Knežević, S.; Ognjanović, M.; Stanković, V.; Zlatanova, M.; Nešić, A.; Gavrović-Jankulović, M.; Stanković, D. La(OH)3 Multi-Walled Carbon Nanotube/Carbon Paste-Based Sensing Approach for the Detection of Uric Acid—A Product of Environmentally Stressed Cells. Biosensors 2022, 12, 705.
72. Negrea, S.; Andelescu, A.A.; Ilies, B.; Motoc, S.; Cretu, C.; Cseh, L.; Rastei, M.; Donnio, B.; Szerb, E.I.; Manea, F. Design of Nanostructured Hybrid Electrodes Based on a Liquid Crystalline Zn(II) Coordination Complex-Carbon Nanotubes Composition for the Specific Electrochemical Sensing of Uric Acid. Nanomater. 2022, 12, 4215.
73. Choukairi, M.; Bouchta, D.; Bounab, L.; González-Romero, E.; Achache, M.; Draoui, K.; Chaouket, F.; Raissouni, I.; Gharous, M. A Carbon Paste Electrode Modified by Bentonite and l-Cysteine for Simultaneous Determination of Ascorbic and Uric Acids: Application in Biological Fluids. ChemistryOpen 2023, 12, e202200201.
74. Xu, J.; Lee, H. Anti-Biofouling Strategies for Long-Term Continuous Use of Implantable Biosensors. Chemosensors 2020, 8, 66.